Mechanistic, Structural, and Spectroscopic Studies on the Catecholase Activity of a Dinuclear Copper Complex by Dioxygen

Enrico Monzani, Giuseppe Battaini, Angelo Perotti, and Luigi Casella*

Dipartimento di Chimica Generale, Università di Pavia, Via Taramelli 12, 27100 Pavia, Italy

Michele Gullotti and Laura Santagostini

Dipartimento CIMA, Centro CNR, Università di Milano, Via Venezian 21, 20133 Milano, Italy

Giorgio Nardin, Lucio Randaccio, and Silvano Geremia

Dipartimento di Scienze Chimiche, Università di Trieste, Via L. Giorgieri 1, 34127 Trieste, Italy

Piero Zanello and Giuliana Opromolla

Dipartimento di Chimica, Università di Siena, Via Pian dei Mantellini 44, 53100 Siena, Italy

Received April 12, 1999

Dinuclear copper(II) complexes with the new ligand 1,6-bis[[bis(1-methyl-2-benzimidazolyl)methyl]amino]-*n*-hexane (EBA) have been synthesized, and their reactivity as models for tyrosinase has been investigated in comparison with that of previously reported dinuclear complexes containing similar aminobis(benzimidazole) donor groups. The complex $[Cu_2(EBA)(H_2O)_4]^{4+}$, five-coordinated SPY, with three nitrogen donors from the ligand and two water molecules per copper, can be reversibly converted into the bis(hydroxo) complex $[Cu_2(EBA)(OH)_2]^{2+}$ by addition of base ($pK_{a1} = 7.77$, $pK_{a2} = 9.01$). The latter complex can also be obtained by air oxidation of $[Cu_2(EBA)]^{2+}$ in methanol. The X-ray structural characterization of $[Cu_2(EBA)(OH)_2]^{2+}$ shows that a double μ-hydroxo bridge is established between the two Cu(II) centers in this complex. The coordination geometry of the coppers is distorted square planar, with two benzimidazole donors and two hydroxo groups in the equatorial plane, and an additional, lengthened and severely distorted axial interaction (∼2.5 Å) with the tertiary amine donor. The small size and the quality of the single crystal as well as the fair loss of crystallinity during data collection required the use of synchrotron radiation at 100 K. $[Cu_2(EBA)(OH)_2][PF_6]_2$: orthorhombic $Pca2_1$ space group, $a = 22.458(2)$ Å, $b = 10.728(1)$ Å, $c = 19.843(2)$ Å, $R = 0.089$. Besides OH^-, the $[Cu_2(EBA)(H_2O)_4]^{4+}$ complex binds azide as a bridging ligand, with the μ-1,3 mode. Azide can also displace μ-OH in $[Cu_2(EBA)(OH)_2]^{2+}$ as a bridging ligand. In general, the binding constants indicate that the long alkyl chain of EBA is less easily folded in the structures containing bridging ligands than the *m*-xylyl residue present in the previously reported dicopper(II) complexes. Electrochemical experiments show that $[Cu_2(EBA)(H_2O)_4]^{4+}$ undergoes a single, partially chemically reversible, two-electron reduction to the corresponding dicopper(I) congener at positive potential values ($E^{0\prime} = 0.22$ V, vs SCE). Interestingly, however, coordination to azide ion makes the reduction process proceed through two separated one-electron steps. The catalytic activity of $[Cu_2(EBA)(H_2O)_4]^{4+}$ in the oxidation of 3,5-di-*tert*-butylcatechol has been examined in methanol/aqueous buffer, pH 5.1. The mechanism of the catalytic cycle parallels that of tyrosinase, where no hydrogen peroxide is released and dioxygen is reduced to water. Low-temperature (−80 °C) spectroscopic experiments show that oxygenation of the reduced complex $[Cu_2(EBA)]^{2+}$ does not produce a stable dioxygen adduct and leads to a μ-oxodicopper(II) species in a fast reaction.

Introduction

In a recent paper[1] we undertook a detailed mechanistic investigation on the catecholase activity of a group of dinuclear copper complexes which are also able to perform regiospecific *ortho* hydroxylation of exogenous phenols and, therefore, act as effective functional models of tyrosinase.[2] From chemical and spectroscopic studies[3] it is known that this enzyme contains a coupled dinuclear copper site with histidine ligation similar to that of hemocyanin, the structure of which is known.[4] Recently, preliminary data on the structure of the catechol oxidase from sweet potatoes (*Ipomoea batatas*) has been

* To whom correspondence should be addressed. Phone: +39-0382-507331. Fax: +39-0382-528544. E-mail: bioinorg@unipv.it.

(1) Monzani, E.; Quinti, L.; Perotti, A.; Casella, L.; Gullotti, M.; Randaccio, L.; Geremia, S.; Nardin, G.; Faleschini, P.; Tabbi, G. *Inorg. Chem.* **1998**, *37*, 553.

(2) Casella, L.; Monzani, E.; Gullotti, M.; Cavagnino, D.; Cerina, L.; Santagostini, L.; Ugo, R. *Inorg. Chem.* **1996**, *35*, 7516.

(3) Solomon, E. I.; Sundaram, U. M.; Machonkin, T. E. *Chem. Rev.* **1996**, *96*, 2563.

(4) Magnus, K. A.; Ton-That, H.; Carpenter, J. E. *Chem. Rev.* **1994**, *94*, 4, 727.

10.1021/ic990397b CCC: $18.00
Published on Web 10/28/1999

reported.[5] This enzyme also contains a coupled dinuclear copper site, with three histidine ligands per copper and, in the oxidized form, an additional hydroxide bridge, but unlike tyrosinase it is only active in the transformation of *o*-diphenols to *o*-quinones and not in the hydroxylation of phenols to diphenols.

While the investigation of dinuclear copper complexes which are active in model hydroxylation reactions at C−H bonds of their ligand has reached considerable detail,[6−9] our understanding of how model dinuclear copper complexes perform dioxygen activation reactions on, e.g., exogenous phenolic substrates is much more limited. The mechanisms of the latter reactions appear clearly more complex at the outset, since a third species besides the copper species and dioxygen, the substrate, comes into play and an active ternary complex may to be formed at some stage. For these reasons, although several complexes have been shown to be active in catecholase reactions,[1,10,11] and in some instances also in phenolase reactions,[1,2] our knowledge of these reactions is limited to general structure−activity patterns and scattered spectral observations. However, the interest in obtaining deeper insight into these and other copper-mediated substrate oxidations is enormous, both from the point of view of gaining a better understanding of the enzymatic reactions and to provide a basis to support further development in the synthesis of new catalysts for selective oxidations.[12]

Here we report new dicopper(II) complexes of the diaminotetrabenzimidazole (N_6) ligand EBA and the investigation of their activity in biomimetic catecholase and phenolase reactions. The ligand 1,6-bis[[bis(1-methyl-2-benzimidazolyl)methyl]-amino]-*n*-hexane (EBA) contains aminobis(benzimidazole) arms of the same type as those of the ligands studied before (e.g., L-55 and L-66),[1,2] but these are supported by an extended aliphatic chain of six methylene carbons instead of the more rigid *m*-xylyl residue previously employed (Chart 1). We expect that this replacement will affect to some extent the properties of the resulting copper complexes, e.g., their redox potential, and therefore also the reactivity pattern in the oxidation reactions. For the present EBA system, for the first time, the true tyrosinase pathway in a catalytic catecholase reaction could be demonstrated.

Chart 1

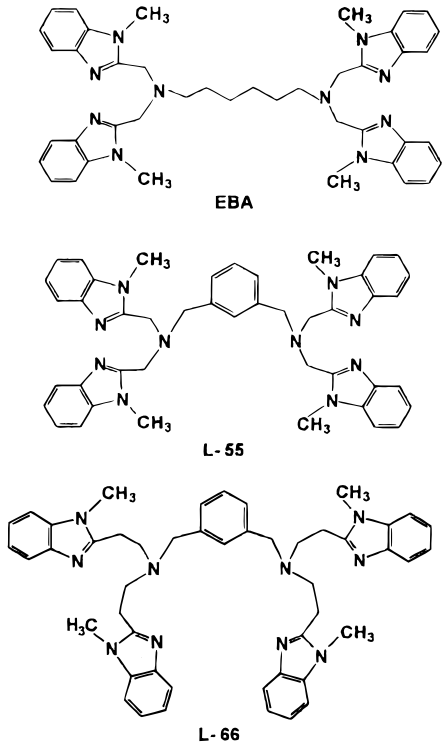

Results and Discussion

Ligand Protonation and Stability Constants of EBA−Copper(II) Complexes. The protonation and complex-forming equilibria with Cu^{2+} of the ligand EBA were investigated potentiometrically in a mixture of acetonitrile−water, 4:1 (v/v). For the six protonation steps of EBA, the cumulative log β values of the formation constants 11.16(0.1), 21.63(0.1), 30.60(0.1), 37.49(0.2), 43.70(0.2), and 49.47(0.3) were found. The ligand easily and simultaneously incorporates two copper(II) ions according to the equilibrium

$$2Cu^{2+} + EBA \rightleftharpoons [Cu_2(EBA)]^{4+} \qquad \log \beta_{120} = 37.68 \quad (1)$$

Successively the complex containing two copper ions, each coordinated to three nitrogen atoms of the ligand and water molecules, undergoes a stepwise deprotonation of coordinated water molecules according to the equilibria

$$[Cu_2(EBA)(H_2O)_2]^{4+} \rightleftharpoons [Cu_2(EBA)(H_2O)(OH)]^{3+} + H^+ \quad (2)$$

with a pK_{a1} of 7.77 and

$$[Cu_2(EBA)(H_2O)(OH)]^{3+} \rightleftharpoons [Cu_2(EBA)(OH)_2]^{2+} + H^+ \quad (3)$$

with a pK_{a2} of 7.01. It can be noted that both pK_a values are rather low and consistent with the formation of bridged μ-hydroxodicopper(II) species. The X-ray crystal structure determination of $[Cu_2(EBA)(OH)_2]^{2+}$ discussed below shows that actually a bis-μ-hydroxo arrangement drives proton dissociation, accounting for pK_{a2} < pK_{a1} in this system. Nevertheless, the monohydroxo species is important because, as is shown in the species distribution diagram in Figure 1, it forms first and assists the formation of the ring-closed $Cu_2(OH)_2$ core.

X-ray Structure of $[Cu_2(EBA)(OH)_2][PF_6]_2$. The crystals consist of binuclear $[Cu_2(EBA)(OH)_2]^{2+}$ cations and PF_6^- anions. An ORTEP drawing,[13] together with the atom numbering scheme of the cation, is shown in Figure 2. The cations have an approximate C_2 symmetry, the 2-fold axis passing through the middle point between the two Cu ions and that between C21 and C22 atoms of the aliphatic chain. The structure of the cation bears some resemblance to that of $[Cu_2L3(OMe)_2]^{2+}$ [L3

(5) Klabunde, T.; Eicken, C.; Sacchettini, J.; Krebs, B. *Nat. Struct. Biol* **1998**, *5*, 1084.
(6) Pidcock, E.; Obias, H. V.; Xin, Zhang, C.; Karlin, K. D.; Solomon, E. I. *J. Am. Chem. Soc.* **1998**, *120*, 7841 and references therein.
(7) Mahapatra, S.; Kaderli, S.; Llobet, A.; Neuhold, Y.-M.; Palanché, T.; Halfen, J. A.; Young, V. G., Jr.; Kaden, T. A.; Que, L., Jr.; Zuberbühler, A. D.; Tolman, W. B. *Inorg. Chem.* **1997**, *36*, 6343 and references therein.
(8) Itoh, S.; Nakao, H.; Berreau, L. M.; Kondo, T.; Komatsu, M.; Fukuzumi, S. *J. Am. Chem. Soc.* **1998**, *120*, 2890.
(9) Ryan, S.; Adams, H.; Fenton, D. E.; Becker, M.; Schindler, S. *Inorg. Chem.* **1998**, *37*, 2134.
(10) See e.g.: Simandi, L. I. *Catalytic Activation of Dioxygen by Metal Complexes*; Kluwer: Dordrecht, The Netherlands, 1992.
(11) Martell, A. E.; Motekaitis, R. J., Menif, R.; Rockcliffe, D. A.; Llobet, A. *J. Mol. Catal., A* **1997**, *117*, 205 and references therein.
(12) (a) Reedijk, J. In *Bioinorganic Catalysis*; Reedijk, J., Ed.; Marcel Dekker: New York, 1993.
(13) Johnson, C. K. *ORTEP*; Report ORNL-5138; Oak Ridge National Laboratory: Oak Ridge, TN, 1976.

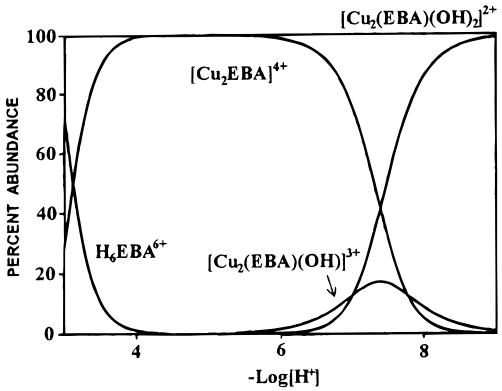

Figure 1. Species distribution in the 2Cu/EBA system as a function of pH in acetonitrile/water solution.

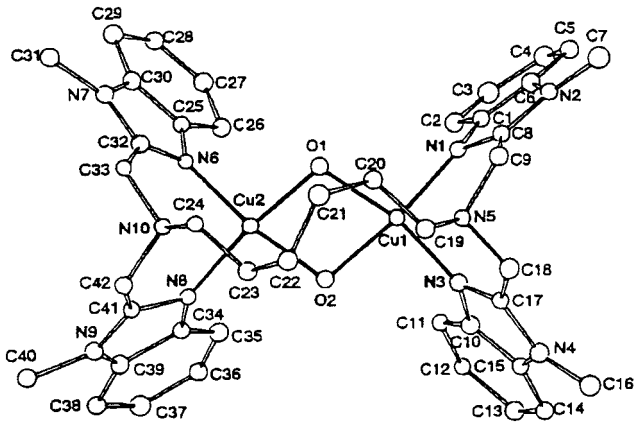

Figure 2. ORTEP diagram of the $[Cu_2(EBA)(OH)_2]^{2+}$ cation with the atom numbering scheme.

$= (2\text{-py}CH_2CH_2)_2N(CH_2)_3N(2\text{-}CH_2CH_2py)_2]$[14] where the L3 ligand has aminobis(pyridyl) arms instead of aminobis(benzimidazolyl) ones and a spacer of three instead of six methylene carbons. As in the L3 derivative, each copper has a distorted square planar geometry and coordinates to the tertiary amine in the apical position and the two sp^2 N donors of the tridentate arm in two cis basal positions. The other two equatorial positions are occupied by the bridging OH^- groups (Figure 2). However, in the EBA derivative the coordination around the metal is dramatically more distorted than in the L3 analogue, because of the large difference in the length of the spacer and the size of the chelate rings. The relative coordination geometries for the two cations are compared in Table 1 together with the length of the spacer (Nterz···Nterz) and the intermetallic distances. In the EBA derivative, the axial Cu−N(sp^3) distances are significantly lengthened by about 0.2 Å and the coordination angles involving the axial N donor more widely deviate from the ideal value of 90° with respect to the L3 derivative (Table 1). This is in agreement with the values of the N(sp^3)···N(sp^3) distance, which are 6.050 and 4.747 Å in EBA and L3 derivatives, respectively.

The basal donors of Cu1 and Cu2 are coplanar within ±0.028(8) and ±0.057(8) Å, respectively, and the displacement of Cu1 and Cu2 out of their respective mean planes are 0.140(7) and 0.173(7) Å, respectively, toward the apical N donor. The two N2O2 basal planes make a dihedral angle, β, of 20.0(2)°, bending on the side opposite the apical ligand, with a butterfly deformation along the O1···O2 line (Figure 3). Consequently,

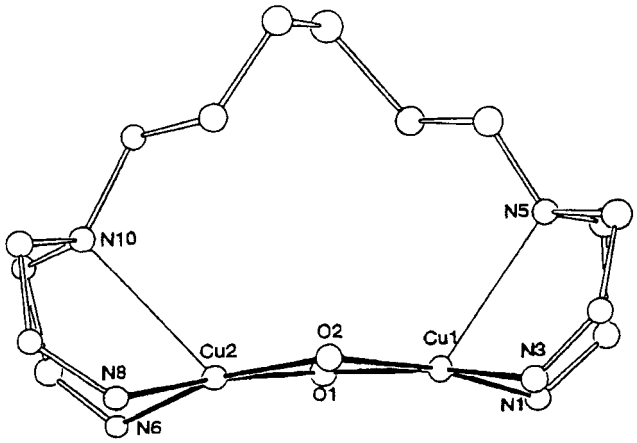

Figure 3. A perspective view of the distorted pyramidal coordination about the copper ions in the $[Cu_2(EBA)(OH)_2]^{2+}$ cation.

Table 1. Comparison of Coordination Bond Lengths and Angles in $[Cu_2((EBA)(OH)_2](PF_6)_2$ and $[Cu_2(L_3)(OMe)_2](ClO_4)_2$

	$[Cu_2(EBA)(OH)_2](PF_6)_2$	$[Cu_2(L3)(OMe)_2](ClO_4)_2$
	Bond Lengths (Å)	
Cu1−O1	1.892(11)	1.934(9)
Cu1−O2	1.941(10)	1.934(9)
Cu1−N1	1.930(12)	1.992(12)
Cu1−N3	1.918(13)	2.004(14)
Cu1−N5	2.487(11)	2.363(13)
Cu2−O1	1.882(10)	
Cu2−O2	1.887(12)	
Cu2−N6	1.942(11)	
Cu2−N8	1.983(12)	
Cu2−N10	2.548(11)	
Cu1···Cu2	2.988(2)	3.070
N5···N10	6.050(15)	4.747
	Bond Angles (deg)	
O1−Cu1−O2	75.2(4)	74.8(5)
O1−Cu1−N1	98.4(5)	96.8(5)
O1−Cu1−N3	165.9(5)	152.2(6)
O1−Cu1−N5	116.2(4)	115.3(5)
O2−Cu1−N1	170.4(5)	168.4(6)
O2−Cu1−N3	92.5(5)	94.1(5)
O2−Cu1−N5	113.0(4)	101.7(6)
N1−Cu1−N3	92.9(5)	91.7(6)
N1−Cu1−N5	76.1(4)	89.0(5)
N3−Cu1−N5	74.7(4)	91.7(6)
Cu1−O1−Cu2	104.7(5)	105.0(7)
Cu1−O2−Cu2	102.6(5)	105.0(6)
O1−Cu2−O2	76.8(5)	
O1−Cu2−N6	94.8(5)	
O1−Cu2−N8	168.8(5)	
O1−Cu2−N10	116.1(4)	
O2−Cu2−N6	166.6(4)	
O2−Cu2−N8	94.5(5)	
O2−Cu2−N10	118.0(4)	
N6−Cu2−N8	92.4(5)	
N6−Cu2−N10	75.0(4)	
N8−Cu2−N10	74.0(4)	

the Cul···Cu2 distance of 2.988(2) Å is one of the shortest among those observed for complexes containing alkoxy and hydroxy doubly bridged dicopper units, in which the intermetallic distances range from 2.995(2)[15] to 3.070(2)[14] Å. A similar bending deformation ($\beta = -32.3°$) and a short Cu···Cu distance (2.995(2) Å) are reported for the more crowded $[Cu_2(L3O^-)(OH)]^{2+}$ cation,[15] where the spacer of the L3 ligand bears a deprotonated RO^- group. On the contrary, smaller values of β (4.2−9.6°) and longer Cu···Cu distances (3.08−3.13 Å) are

(14) Karlin, K. D.; Shi, J.; Hayes, J. C.; McKown, J. W.; Hutchinson, J. P.; Zubieta, J. *Inorg. Chim. Acta* **1984**, *91*, L3.

(15) Karlin, K. D.; Sanyal, I.; Farooq, A.; Jacobson, R. J.; Shaik, S. N.; Zubieta, J. *Inorg. Chim. Acta* **1990**, *174*, 13.

Chart 2

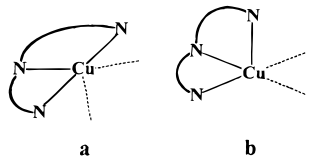

a b

Chart 3

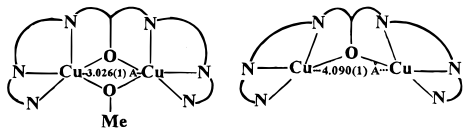

a b

reported in other similar dicopper cations.[16] It is of interest to stress a peculiarity of the polydentate ligands characterized by two tridentate arms and a spacer either bearing, such as L3O$^-$, or not bearing, as in EBA, a further coordinating group. Each arm can coordinate to a metal center essentially in two ways. In one, the whole arm assumes an approximately planar arrangement (Chart 2a), in the other a nonplanar arrangement (Chart 2b). The latter can be called a "folded" arrangement, the former a "planar" arrangement. Inspection of the reported structures of dinuclear copper cations containing such kind of ligands indicates that, upon coordination to two copper ions, closely held at about 3.0 Å by alkoxy or hydroxy double bridges, the folded arrangement of the ligand occurs as in the above cited dinuclear species.[14−16] This arrangement is also found in singly bridged dinuclear cations,[17] where the two Cu(II) ions are far apart by 3.5 Å. When the two metal centers are far apart by more than about 4.5 Å, even if the polypodal ligand contains an internal O bridge, the planar arrangement is observed.[18] The comparison of the structures $[Cu_2(bimp)(OMe)][ClO_4]_2$ (Chart 3a) and $[Cu_2(bimp)(MeOH)_2][ClO_4]_3$ (Chart 3b) (bimp = 2,6-bis[(bis((1-methylimidazol-2-yl)methyl)amino)methyl]-4-methylphenolate) suggests that the crossover point between the folded and planar arrangements is close to a Cu···Cu distance of about 4.0 Å. In fact, in Chart 3a the folded arrangement corresponds to a Cu···Cu of 3.026(1) Å. In Chart 3b the Cu···Cu distance is 4.090(1) Å and the arrangement of the polypodal ligands is intermediate between the planar and folded conformations.[19] Therefore, in the case of the EBA derivative, the pH-dependent interconversion between $[Cu(EBA)]^{4+}$ and $[Cu(EBA)(OH)_2]^{2+}$ should be accompanied by a gradual rearrangement of the polypodal ligand from the planar to the folded arrangement and vice versa and a significant rearrangement of donor geometry about the copper ions.

Characterization and Ligand-Binding Properties of EBA Complexes. The IR spectrum of $[Cu_2(EBA)][ClO_4]_4\cdot 4H_2O$ recorded as a Nujol mull exhibits a strong peak at 3538 cm^{-1} and a medium-intensity peak at 1653 cm^{-1}, attributable to OH stretching and HOH bending modes of coordinated water, respectively. When the IR spectrum is recorded in a KBr pellet, the high-energy peak becomes broader and shifts to 3440 cm^{-1}, while the bending peak disappears and is replaced by a broad feature under the aromatic CH stretching vibration at 1618 cm^{-1}. For the bis(hydroxo) complex $[Cu_2(EBA)(OH)_2][PF_6]_2$ a pair of IR bands attributable to OH stretching occurs at 3668 and 3598 cm^{-1}, the former of which has higher intensity. We noted previously[20] that ν(OH) shifts to higher frequency when coordinated water is replaced by bridging OH in dinuclear Cu(II) complexes. This effect may be interpreted by the "hardening" of the OH bond when this group is bound to adjacent metal ions.[21] Support for the presence of a pair of coordinated water molecules per copper in the Cu_2−EBA complex, which should therefore be formulated as $[Cu_2(EBA)(H_2O)_4]^{4+}$, comes from ESI-MS spectrum of the sample, which shows a small cluster of peaks centered at *m*/*z* 1187.0, which corresponds to the cation $\{[Cu_2(EBA)(H_2O)_4](ClO_4)_3\}^+$, together with a prominent cluster of peaks centered at *m*/*z* 1117.0 corresponding to $\{[Cu_2(EBA)](ClO_4)_3\}^+$. The intensity distribution of the peaks within the clusters was in perfect agreement with the simulated spectra.

The electronic spectra of $[Cu_2(EBA)(H_2O)_4]^{4+}$ and $[Cu_2(EBA)(OH)_2]^{2+}$ differ markedly in the near-UV region above ∼290 nm and in the visible region, while the higher energy UV spectrum is dominated by similar intraligand absorptions. For the former complex, the near-UV spectrum in MeOH/MeCN features two resolved shoulders near 350 nm (ϵ 1000 M^{-1} cm^{-1}) and 300 nm (ϵ 2200 M^{-1} cm^{-1}), due to π(benzimidazole) → Cu(II) LMCT[20,22] and σ(amino) → Cu(II) LMCT[23] transitions, respectively. The broad but symmetric d−d band at 675 nm suggests that the geometry about the Cu(II) ions is best described as square pyramidal.[24] The spectrum is somewhat solvent dependent, indicating that solvent molecules displace coordinated water. For the hydroxo complex $[Cu_2(EBA)(OH)_2]^{2+}$ two moderately strong bands at 310 nm (ϵ 5100 M^{-1} cm^{-1}) and 354 nm (ϵ 6500 M^{-1} cm^{-1}) dominate the near-UV−vis spectrum, while an asymmetric d−d band occurs at low energy, with a maximum at 610 nm (ϵ 180 M^{-1} cm^{-1}) and a shoulder at 550 nm (ϵ 170 M^{-1} cm^{-1}). The shift to higher energy of the d−d bands, from $[Cu_2(EBA)]^{4+}$ to $[Cu_2(EBA)(OH)_2]^{2+}$, is in agreement with the change to a basic square planar stereochemistry of the Cu(II) ions, with strongly distorted apical amine interaction in the latter, as discussed above. The pair of near-UV bands bear features similar to those described previously for the bis(hydroxo)dicopper(II) complexes derived from L-55 and L-66, and are attributed to OH$^-$ → Cu(II) LMCT transitions originating in the dibridged $Cu_2(OH)_2$ core.[20] The presence of the double hydroxide bridge in the complex produces strong electronic coupling between the Cu(II) ions, and in fact $[Cu_2(EBA)(OH)_2]^{2+}$ is EPR silent in frozen solution. For $[Cu_2(EBA)]^{4+}$ the frozen solution EPR spectrum exhibits a signal for monomeric Cu(II) species, indicating that the two Cu(II) centers are far apart in the complex. The EPR parameters, $g_{\|} = 2.273$, $g_{\perp} = 2.077$, and $|A_{\|}| = 144 \times 10^{-4}$ cm^{-1}, are quite similar to those of other copper(II) complexes with ligands containing similar tridentate aminobis(benzimidazole) units and five-coordinate structure, previously reported by us, and confirm the stereochemical propensity of these Cu(II) sites.

The complex $[Cu_2(EBA)(OH)_2]^{2+}$ was conveniently isolated as PF_6^- salt upon air oxidation of the dicopper(I) complex. However, $[Cu_2(EBA)(H_2O)_4]^{4+}$ and $[Cu_2(EBA)(OH)_2]^{2+}$ can be

(16) Karlin, K. D.; Farooq, A.; Hayes, J. C.; Cohen, B. I.; Rowe, T. M.; Sinn, E.; Zubieta, J. *Inorg. Chem.* **1987**, *26*, 1271.
(17) Mahroof-Tahir, M.; Murthy, N. N.; Karlin, K. D.; Backburn, N. J.; Shaikh, S. N.; Zubieta, J *Inorg. Chem.* **1992**, *31*, 3001
(18) Zeug, W. F.; Cheng, C. P.; Wong, S. M.; Lee, G. *Inorg. Chem.* **1996**, *35*, 2259.
(19) Oberhausen, K. J.; Richardson, J. F.; Buchanan, R. M.; McCusker, J. K.; Hendrickson, D. N.; Latour, J. *Inorg. Chem.* **1991**, *30*, 1337.
(20) Casella, L.; Carugo, O.; Gullotti, M.; Garofani, S.; Zanello, P. *Inorg. Chem.* **1993**, *32*, 2056.
(21) Lutz, H. D.; Heming, J.; Maeuseter, H. *J. Mol. Struct.* **1987**, *156*, 143.
(22) Dagdigian, J. V.; McKee, V.; Reed, C. A. *Inorg. Chem.* **1982**, *21*, 1332.
(23) Lever, A. B. P. *Inorganic Electronic Spectroscopy*, 2nd ed.; Elsevier: Amsterdam, 1984; p 355.
(24) Hathaway, B. J. *Struct. Bonding* **1984**, *57*, 55.

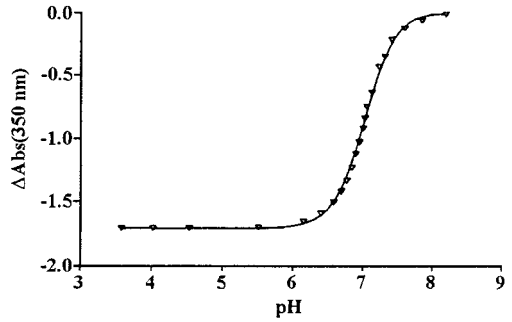

Figure 4. Absorbance variation at 350 nm vs pH in the titration of $[Cu_2(EBA)(OH)_2]^{2+}$ (86 μM) with perchloric acid in MeCN/MeOH/H_2O, 6:3:1 (v/v/v). The pH values were obtained by Gran's method.

Scheme 1

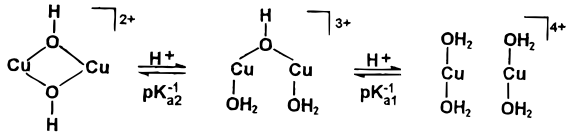

fully interconverted in solution by the addition of base and acid, respectively. Spectral titrations carried out in a mixed solvent of MeCN/MeOH/H_2O, 6:3:1 (v/v/v) (for solubility reasons), show that the interconversion occurs in two nonseparable steps (no isosbestic points), so that two consecutive dissociation equilibria can be written (Scheme 1). This behavior contrasts with that observed for L-55 and L-66 complexes where the bis(hydroxo) species formed in a single step.[20] An estimation of the two pK_a values for the protonation processes was obtained by plotting the absorbance change at 350 nm vs pH (Figure 4). The curve could be fitted by the equation resulting from the assumption of two nonseparable protonation steps (see the Supporting Information):

$$\Delta A_{350\ nm} = \frac{\Delta\epsilon_b[complex]K_{a2}^{-1}[H^+] + \Delta\epsilon_a[complex]K_{a2}^{-1}K_{a1}^{-1}[H^+]^2}{1 + K_{a2}^{-1}[H^+] + K_{a2}^{-1}K_{a1}^{-1}[H^+]^2} \quad (4)$$

where $\Delta\epsilon_b$ is the difference in extinction coefficients between the monohydroxide complex and the bishydroxide complex, while $\Delta\epsilon_a$ is the difference in extinction coefficients between $[Cu_2(EBA)(H_2O)_4]^{4+}$ and $[Cu_2(EBA)(OH)_2]^{2+}$. The estimated values of the two constants are p$K_{a1} = 8.2 \pm 0.5$ and p$K_{a2} = 6.0 \pm 0.5$, in reasonable agreement with the potentiometric data, taking into account the different solvent used. The lower value of pK_{a2} indicates that deprotonation of the second water molecule is facilitated by the presence of the hydroxide bridge, despite the reduced positive charge in the complex.

Since the $[Cu_2(EBA)]^{4+}$ complex seems available to adopt a closed conformation in the presence of small anionic ligands that can form intramolecular bridges between the Cu(II) ions, we investigated the binding of azide to this complex, since bridging azide can be easily recognized by its characteristic spectral behavior.[20] The isolated adduct $[Cu_2(EBA)(N_3)(H_2O)_2]^{3+}$, in fact, exhibits IR and UV−vis spectral features in agreement with the presence of a bridging azide and one bound water to each Cu(II) (sharp IR peaks at 3618 and 3541 cm^{-1}) to support five-coordination at the metal centers. The azide asymmetric stretching occurs at 2048 cm^{-1} in the IR spectrum and shifts to 2036 cm^{-1} without splitting in the adduct prepared

Scheme 2

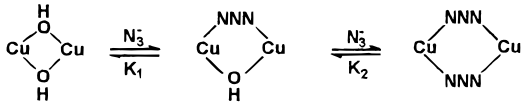

with unsymmetrically labeled azide ($^{15}N^{14}N^{14}N$). This behavior indicates that azide acts as a μ-1,3 bridging ligand in the adduct.[20,26] The near-UV band attributable to π(azide) → Cu(II) LMCT transition shows a multicomponent structure and solvent dependence, as we found previously for the corresponding dicopper(II) complexes of L-55 and L-66.[20] For $[Cu_2(EBA)(N_3)]^{3+}$ we find the stronger high-energy component at 362 nm in MeOH and 395 nm in MeCN and the weaker low-energy component at 440 nm in MeOH and 490 nm in MeCN. As observed previously, [20] a distinct azide LMCT band at such low energy has been observed only in the spectrum of some met-azide hemocyanins. [26,27]

A spectrophotometric titration of $[Cu_2(EBA)]^{4+}$ with azide in MeOH/MeCN, 9:1, enabled the binding constant to be estimated, since in the initial phase, up to about $[N_3]:[Cu_2] \approx 1:1$, isosbestic points at 293 and 316 nm were maintained during the growth of the LMCT band (at 366 nm). At higher azide concentrations the isosbestic points were lost due to the binding of further azide molecules. The binding constant of the first azide, obtained by fitting of the titration data at 366 nm, yields $K = 2.3 \times 10^4\ M^{-1}$. This value is appreciably lower than those previously found for the parent $[Cu_2(L\text{-}55)]^{4+}$ and $[Cu_2(L\text{-}66)]^{4+}$ complexes,[21] indicating that the long EBA alkyl chain has more difficulty than the *m*-xylyl residue folding into the closed conformation required to hold the bridging Cu−N_3−Cu unit, as shown in structure I.

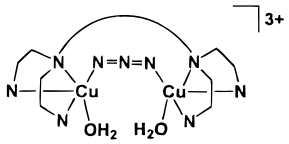

Structure I

Azide binding experiments were also performed on the bis(hydroxo) complex $[Cu_2(EBA)(OH)_2]^{2+}$, but for solubility reasons the titrations had to be carried out in a solution of MeOH/MeCN, 1:1. The addition of azide produces a decrease of the LMCT bands of the hydroxo bridges and the growth of a broad absorption near 430 nm. Unlike for the xylyl complexes,[20] the titration proceeds without holding any isosbestic point, indicating that substitution equilibria of the first and second hydroxide bridges by azide cannot be separated (Scheme 2).

An analysis of the titration data according to a procedure similar to that employed for the proton dissociation equilibria and described in the Supporting Information leads to an estimate of $K_1 = 1850\ M^{-1}$ and $K_2 = 410\ M^{-1}$. These values are both higher than those found for K_1 for azide binding to $[Cu_2(L\text{-}55)(OH)_2]^{2+}$ and $[Cu_2(L\text{-}66)(OH)_2]^{2+}$, due only in part to the decreased polarity of the solvent mixture employed here.[28] The relative ease with which replacement of particularly the second

(25) Casella, L.; Carugo, O.; Gullotti, M.; Doldi, S.; Frassoni, M. *Inorg. Chem.* **1996**, *35*, 1101.
(26) Pate, J. E.; Ross, P. K.; Thamann, T. J.; Reed, C. A.; Karlin, K. D.; Sorrell, T. N.; Solomon, E. I. *J. Am. Chem. Soc.* **1989**, *111* (1), 5198.
(27) Beltramini, M.; Bubacco, L.; Casella, L.; Alzuet, G.; Gullotti, M.; Salvato, B. *Eur. J. Biochem.* **1995**, *232*, 98.
(28) Casella, L.; Gullotti, M.; Pallanza, G.; Buga, M. *Inorg. Chem.* **1991**, *30*, 221.

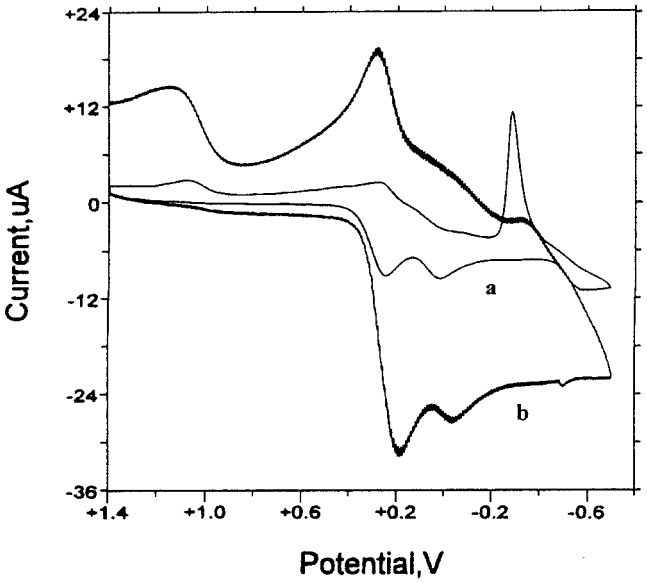

Figure 5. Cyclic voltammetric responses recorded at a platinum electrode on a MeCN solution of $[Cu_2(EBA)(H_2O)_4]^{4+}$ (1.1×10^{-3} M). Scan rates: (a) 0.05 V s^{-1}; (b) 0.5 V s^{-1}. $[NEt_4]PF_6$ (0.1 M) supporting electrolyte.

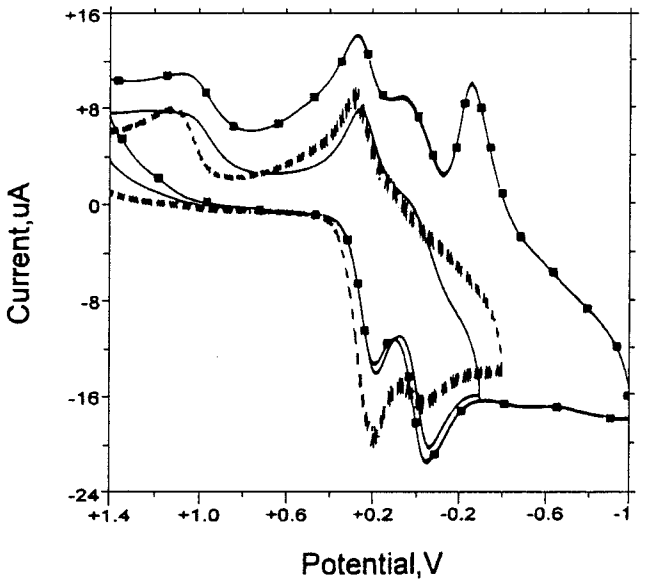

Figure 6. Cyclic voltammetric responses recorded at a platinum electrode on a MeCN solution of $[Cu_2(EBA)(H_2O)_2]^{4+}$ (1.1×10^{-3} M) upon addition of increasing amounts of NaN_3. $[Cu_2]^{4+}$:$[N_3]^-$ ratios: 1:0 (- - -); 1:10 (—); 1:25 (■). $[NEt_4]PF_6$ (0.1 M) supporting electrolyte. Scan rate 0.2 V s^{-1}.

hydroxide bridge occurs here suggests that the process may be driven by relaxation of the EBA alkyl chain, which gains conformational mobility as the μ-1,1 hydroxo bridges are replaced by the longer μ-1,3 azide bridges.

Electrochemistry. Figure 5 illustrates the cyclic voltammetric behavior of an acetonitrile solution of the dicopper(II) complex $[Cu_2(EBA)(H_2O)_4]^{4+}$ at either low or relatively high scan rates. The tetracation undergoes a main, partially chemically reversible reduction process ($E^{\circ\prime} = +0.22$ V), which generates a side species, which in turn undergoes an irreversible reduction at $E_p = +0.02$ V. Controlled potential coulometric tests in correspondence to the first cathodic step ($E_w = +0.1$ V) show the consumption of 1.6−1.7 electrons/molecule. The original blue solution turns colorless upon exhaustive reduction, and cyclic voltammetry only displays the reduction of the above-mentioned byproduct. We assume that this first step involves in reality the single two-electron process $Cu^{II}Cu^{II}/Cu^{I}Cu^{I}$, the closeness of the second step making notably long the time needed for completion of the coulometric test. The cyclic voltammetric profiles prove that the chemical complication following the two-electron addition not only leads to the unknown species responsible for the second reduction step but also involves decomplexation and release of Cu^+ ion, which, in turn, undergoes either the Cu^+/Cu^0 reduction ($E_p = -0.6$ V), as pointed out by the appearance at low scan rate of the anodic stripping of the electrodeposed Cu(0) in the back-scan, or the Cu^+Cu^{2+} oxidation ($E_p = +1.1$ V).[29] It is likely that the lack of the expected $Cu^{I}Cu^{I}/Cu^{0}Cu^{0}$ step(s) (up to −1.9 V) might be due just to the complete destruction of the dinuclear molecular frame. The occurrence of a single two-electron reduction testifies that no electronic interaction exists between the two copper(II) centers.

It is useful to take into account that the related mononuclear $[Cu(2\text{-}BB)]^{2+}$ dication[25] undergoes a chemically reversible Cu^{II}/Cu^{I} reduction at $E^{\circ\prime} = +0.22$ V, followed by the irreversible Cu^{I}/Cu^{0} reduction at $E_p = -0.87$ V (Figure S1, Supporting Information). Interestingly, the potential value of the Cu^{II}/Cu^{I} reduction in the mononuclear complex is just coincident with that of the corresponding step in the dinuclear complex, even if in the latter the electron addition generates the kinetically unstable dicopper(I) congener. It seems thus conceivable that the favored Coulombic effects of adding electrons to the dicopper tetracation with respect to the monocopper dication are compensated by the increased steric strains of the aliphatic bridging chain.

Moving to the dication $[Cu_2(EBA)(OH)_2]^{2+}$, its low solubility in MeCN prevented an accurate analysis of its redox propensity as far as the number of electrons involved in the redox changes is concerned (Figure S2, Supporting Information). As a matter of fact, it undergoes two separated reductions (the first one at $E^{\circ\prime} = +0.16$ V having features of chemical reversibility, the second one at $E_p = -0.85$ V being irreversible in character), followed by the third reduction to copper metal (at $E_p = -1.18$ V).

In view of the spectrophotometrically ascertained binding ability of N_3^- ions toward $[Cu_2(EBA)(H_2O)_4]^{4+}$, we followed such a complexation process electrochemically. Figure 6 summarizes the relevant results. Despite the troubling presence of the previously discussed second reduction step of $[Cu_2(EBA)(H_2O)_4]^{4+}$, it seems rather easy to realize that upon addition of azide ions the cathodic process progressively passes from a primary single two-electron $Cu^{II}Cu^{II}/Cu^{I}Cu^{I}$ reduction to two separated $Cu^{II}Cu^{II}/Cu^{II}Cu^{I}/Cu^{I}Cu^{I}$ one-electron reductions. As a matter of fact, the current of the original process gradually decreases in favor of that of the second step (which differs from that due to the original chemical complication) until they reach an almost equal intensity. A detailed examination of either the potential values or the current values resulting from the addition of azide ions supports such an assumption (Table S1, Supporting Information). It is interesting to note how in reality the complexation process is not stoichiometric but governed by an equilibrium reaction. As a matter of fact, only high $[N_3]^-/[Cu_2]^{4+}$ ratios make the association reaction complete in solution.

On the basis of the separation of the two one-electron additions, $\Delta E^{\circ\prime} = 0.23$ V, a comproportionation constant, K_{com},

(29) Cinquantini, A.; Cini, R.; Seeber, R.; Zanello, P. *J. Electroanal. Chem.* **1981**, *121*, 301.

Scheme 3

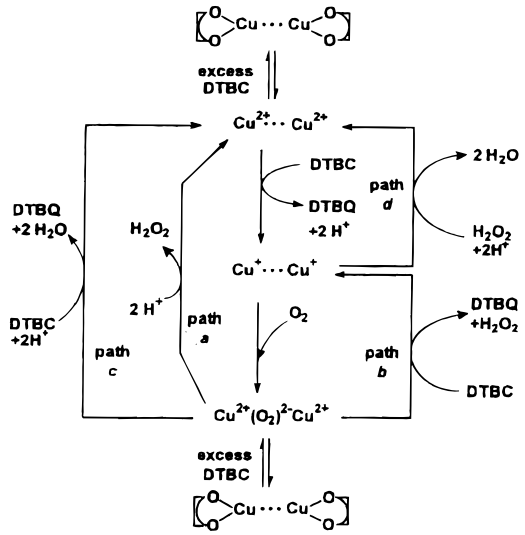

of about 50 can be computed for the $Cu^{II}-N_3-Cu^{II}/Cu^{I}-N_3-Cu^{I}$ interaction, which allows the mixed-valent $Cu^{II}-N_3-Cu^{I}$ adduct to be classified at the borders of a localized and slightly delocalized species. This means that, despite the appearance of two separated one-electron reductions, the N_3^- bridging does not significantly improve the communication between the two copper sites. In contrast, if allowance is made to interpret the redox profile of $[Cu_2(EBA)(OH)_2]^{2+}$ as due to two separated one-electron reductions (followed by a further single two-electron reduction), a K_{com} of about 2×10^7 can be calculated, which would testify to a completely delocalized $Cu^{II}-(OH)_2-Cu^{I}$ mixed-valent species, i.e., the occurrence of strong communication between the two copper centers.

Catechol Oxidase Activity. Among the different catechols used in model studies,[1,10,11] 3,5-di-*tert*-butylcatechol (DTBC) is the most widely used substrate due to its low redox potential, which makes it easy to oxidize to the quinone (DTBQ), and its bulky substituents, which make further oxidation reactions such as ring opening slower. Our previous studies on the catalytic oxidation of DTBC, performed with several dicopper(II) complexes including L-55 and L-66,[1,30] have shown that the reaction is biphasic. After a fast stoichiometric step, a slower catalytic reaction occurs. While the rate of the first step always depends on the substrate concentration in a saturating fashion, the rate dependence of the second step on substrate concentration varies with the complex used. Moreover, the addition of hydrogen peroxide was shown to affect the reaction rates, again in a way that depends on the catalyst. The results were explained considering several possible kinetic pathways, summarized in Scheme 3. Hydrogen peroxide was not accumulated during the catalytic cycle, indicating that the kinetic cycle involved either path *c* or both path *b* and an efficient path, *d*.

When the reaction of $[Cu_2(EBA)]^{4+}$ with DTBC was performed in the mixed solvent methanol/aqueous 50 mM phosphate buffer (pH 5.1) saturated with atmospheric oxygen, two phases were observed, as for the related complexes. After a first, fast stoichiometric phase a slower catalytic phase follows. Since the rates of these two steps are not too different, they are difficult to separate. A kinetic equation for two consecutive steps in the catalytic cycle has therefore been derived (see the Supporting Information):

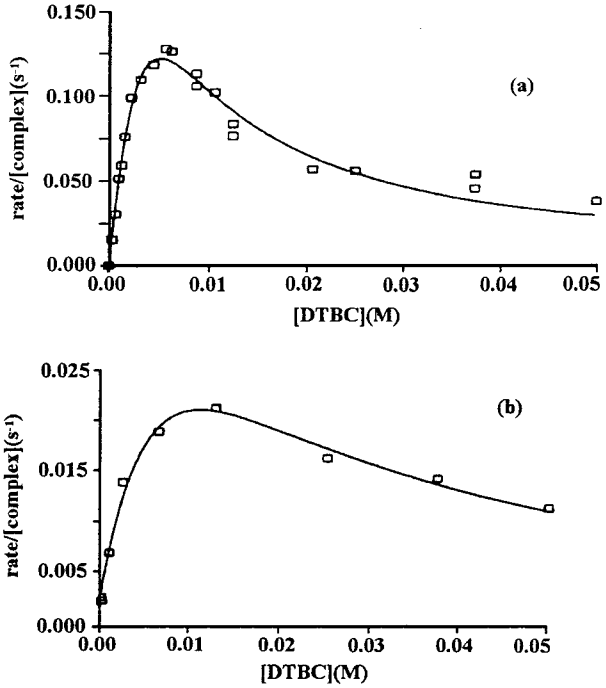

Figure 7. Dependence of the DTBC oxidation rate (a) in the first phase and (b) in the second phase on DTBC concentration using $[Cu_2(EBA)]^{4+}$ (14 μM) as catalyst. The reactions were performed at 20 ± 0.1 °C in a 30:1 mixture of methanol/aqueous phosphate buffer (50 mM), pH 5.1.

$$[\mathrm{DTBQ}] = \frac{r_1[\mathrm{Cat}]}{r_1 + r_2}\left\{\frac{2r_1 t}{[\mathrm{Cat}]} + \frac{r_1 - r_2}{r_1 + r_2}\left[1 - \exp\left(-\frac{r_1 + r_2}{[\mathrm{Cat}]}t\right)\right]\right\} \quad (5)$$

where [Cat] represents the concentration of the catalyst while r_1 and r_2 are the initial rates of the first and second phases, respectively. The rates of both steps depend on the catechol concentration as shown in Figure 7. They cannot be described using a simple kinetic scheme involving a preequilibrium, since the observed velocities do not reach a plateau at high substrate concentration; instead, in the latter conditions substrate inhibition is observed. This behavior can be explained by considering that, in the presence of a large excess of DTBC, coordination of two molecules of DTBC to the complex occurs, each one chelating to a single metal center. The two copper ions are forced to stay far apart in this bis(adduct), preventing the possibility of the two-electron oxidation process to a bridged catecholate that likely yields DTBQ. Interpolation of the rate data could be, in fact, obtained by considering the possibility for the complex to form a 2:1 inactive adduct with DTBC according to the simplified mechanism reported in Scheme 4, where Cat represents the catalyst, in the form of either $Cu^{II}-Cu^{II}$ or $Cu^{II}-O_2^{2-}-Cu^{II}$, and K_C is the catechol binding constant for the bis-(adduct). Considering initial rates and the catechol in large excess, the kinetic treatment gives the following equation:

$$r = \frac{k_{cat}[\mathrm{DTBC}][\mathrm{Cat}]}{K_M(1 + K_C[\mathrm{DTBC}]^2) + [\mathrm{DTBC}]} \quad (6)$$

Table 2 reports the estimated parameters obtained applying eq 6 to the data of Figure 7. Interestingly, while the k_{cat} parameter for the EBA complex is lower than that obtained for the L-55 complex in the same conditions,[1] K_M is significantly

(30) Monzani, E.; Casella, L.; Zoppellaro, G.; Gullotti, M.; Pagliarin, R.; Bonomo, R. P.; Tabbì, G.; Nardin, G.; Randaccio, L. *Inorg. Chim. Acta* **1998**, *282*, 180.

Scheme 4

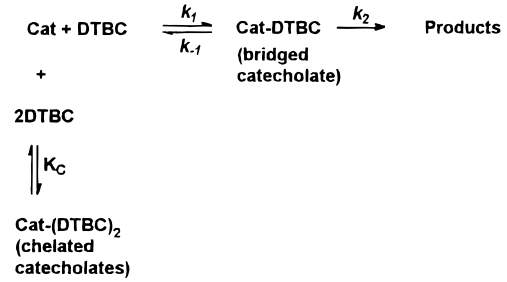

Table 2. Kinetic Parameters for the Catalytic Oxidation of DTBC by $[Cu_2((EBA)]^{4+}$ in Methanol/Aqueous Buffer, pH 5.1, at 20 °C

	first step	second step
k_{cat} (s^{-1})	0.7 ± 0.4	0.05 ± 0.01
k_{cat}/K_M ($M^{-1}\ s^{-1}$)	60 ± 5	7 ± 1
K_M (mM)	13 ± 8	7 ± 2
K_C (M^{-2})	$38\,000 \pm 3000$	8000 ± 1000

larger, thus reducing by more than an order of magnitude the efficiency of the former complex at low DTBC concentration. Since K_M is associated with the capability of the complex to form a 1:1 adduct with the substrate, a large value indicates that formation of a bridged catecholate is more difficult for the EBA complex than for the L-55 complex, in agreement with the azide binding behavior of the two complexes. This interpretation is supported by the finding that comparing the data for the two steps in Table 2, the EBA complex exhibits a reduced tendency to form the bis catecholate adduct (lower K_C value, implying weaker inhibition) and increased tendency to form a bridged catecholate adduct (lower K_M) in the active species of the second step of the reaction, where the two copper ions are already forced to stay close to each other by the dioxygen bridge (Cu_2O_2).

Hydrogen peroxide affects the oxidation of DTBC by $[Cu^{II}_2(EBA)]^{4+}$. In the first phase this effect is almost negligible, whereas on increasing the H_2O_2 concentration the rate of the second step progressively decreases. A similar behavior was exhibited by the copper complex of L-55 and can be interpreted considering that the reaction of the fully reduced complex with dioxygen is very fast, so that the $Cu^I\cdots Cu^I$ species is not accumulated and does not react with peroxide. The reduction in the observed rate is probably due to the reaction (reverse of path *a*)

$$Cu^{II}\cdots Cu^{II} + H_2O_2 \rightarrow Cu^{II}-O_2^{2-}-Cu^{II} + 2H^+ \qquad (7)$$

which transforms the more reactive dicopper(II) species into the less reactive dioxygen adduct.

To clarify whether the turnover cycle involves path *c* or a combination of paths *b* and *d*, the assay based on I_3^-, formed by oxidation of an excess of iodide, was used, the reaction being accelerated by small amounts of lactoperoxidase (LPO).[1] When the oxidation of catechol (6 mM, close to the concentration that maximizes the rates) by $[Cu_2(EBA)]^{4+}$ is performed in the presence of saturating iodide and LPO, formation of the quinone proceeds as in the absence of I^-, while the formation of I_3^- does not differ from that observed in blank experiments (without catalyst and catechol). Thus, iodide does not interfere with the catechol oxidation, and hydrogen peroxide is not accumulated in the system in a detectable amount. The absence of hydrogen peroxide is not due to continuous consumption of the oxidant in the reoxidation of copper(I), according to path *d* in Scheme 3, since under anaerobic conditions and in the presence of LPO, $[Cu_2(EBA)]^{2+}$ and iodide, hydrogen peroxide oxidizes iodide, leaving copper in the reduced form. Since H_2O_2 prefers to react in the $LPO-H_2O_2-I^-$ system than in the reaction shown in path *d*, its absence in the catecholase reaction indicates that path *b* is not involved in the catalytic turnover and the real cycle involves path *c*, the tyrosinase cycle. This mechanism is confirmed by the measurement of dioxygen consumption in the catalytic reaction, which corresponds to the stoichiometry 2 catechol:1 O_2.

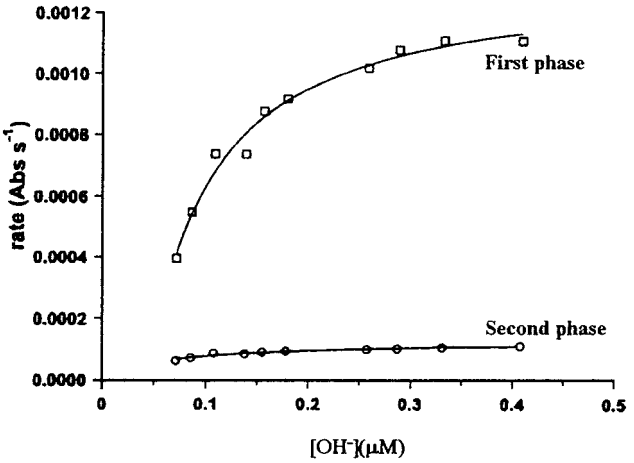

Figure 8. Dependence of the rate (as absorbance change at 396 nm vs time) of the first and second phases of catalytic oxidation of DTBC on the solution pH. The concentration of $[Cu_2(EBA)]^{4+}$ was 14 μM while that of DTBC was 6 mM in all experiments. The reactions were performed at 20 ± 0.1 °C in a 30:1 mixture of methanol/aqueous phosphate buffer (50 mM); the pH of the buffer used was varied from 3.4 to 5.3, and the exact value was controlled by Gran's method.

The pH dependence of the rate for the two phases of the catalytic reaction was also studied, using the solvent mixture of methanol/aqueous buffer, 30:1 (v/v), but changing the pH of the buffer (we preferred to analyze the acidic pH range to prevent problems of substrate autoxidation and to increase the pH sensitivity; see below). The exact pH in the mixed solvent was obtained by calibrating the electrodes according to Gran's method.[31] The reactions were studied using both a substrate concentration that gives the highest rate (6.0 mM) and at a substrate concentration one-fourth of this value. Interestingly, while at the lower catechol concentration the dependence of the rate vs pH is negligible, at high substrate concentration the reaction rates in both phases increase with pH with a saturation behavior (Figure 8). The base (OH^-) affects the rates in different ways since (a) it facilitates the coordination of the substrate by increasing the concentration of its anionic form, (b) the catalyst is present in solution in its aquo or dihydroxo form depending on the pH, and (c) a protonation step can be present also after the coordination of the substrate to the complex.

Low-Temperature Spectroscopy. When solutions of $[Cu_2(EBA)]^{2+}$ in acetone are oxygenated at −78 °C, a moderately intense LMCT band at 350 nm (ϵ 6500 $M^{-1}\ cm^{-1}$) and a weaker band (d−d envelope) at 550 nm ($\epsilon \approx 300\ M^{-1}\ cm^{-1}$) developed quickly. The reaction is complete in minutes ($t_{1/2} = 25$ s, $k_{obs} = 0.028\ s^{-1}$) and cannot be reversed by application of a vacuum, even upon mildly warming the solution. The UV band is bleached by the addition of a small excess of acid at low temperature, but no hydrogen peroxide is detected using either the I_3^- assay or the peroxidase/ABTS assay employed to probe

(31) Gran, G. *Analyst (London)* **1952**, *77*, 661.

the peroxide adduct $[Cu_2(L\text{-}66)(O_2)]^{2+}$.[32] Thus, the reaction of $[Cu_2(EBA)]^{2+}$ with O_2 does not yield a stable dioxygen complex but leads to an oxidized copper(II) species. The spectral characteristics of this species are different from those of the bis(hydroxo)dicopper(II) complex, i.e., the species obtained by air oxidation of $[Cu_2(EBA)]^{2+}$ in methanol and the common end product of several $Cu(I)_2 + O_2$ reactions,[20,33,34] and indicate it is a μ-oxodicopper(II) complex (from the position of the LMCT band),[35] which is formed in a fast reaction from the putative Cu_2O_2 intermediate:

$$Cu(I)\cdots Cu(I) + O_2 \rightarrow [Cu_2O_2] + Cu(I)\cdots Cu(I) \rightarrow 2Cu(II)-O-Cu(II) \quad (8)$$

The extreme electrophilicity of the dioxygen intermediate $[Cu_2O_2]$ is not unexpected in view of the structural features of $[Cu_2(EBA)(OH)_2]^{2+}$ (Figure 3). The very weak and distorted N−Cu (axial) interaction provided by the tertiary amine donor of the ligand to each Cu makes the donor environment provided by EBA practically limited to two poorly basic benzimidazole nitrogens per copper. The situation is likely similar in the dioxygen intermediate (whether a peroxodicopper(II) or a bis-(μ-oxo)dicopper(III) species),[36,37] because it depends on the small size of the adjacent chelate rings provided by the aminobis(benzimidazole) units of the ligand. The oxygenation behavior of $[Cu_2(L\text{-}55)]^{2+}$, where the copper environment is analogous to that of $[Cu_2(EBA)]^{2+}$, is in fact similar. By contrast, with $[Cu_2(L\text{-}66)]^{2+}$, where the larger size of the chelate rings allow a "normal" tridentate coordination at each Cu center, a stable and fully reversible dioxygen adduct is formed at low temperature, and this performs both phenolase and catecholase reactions.[32]

Conclusion

The chemistry of the dicopper complexes derived from the ligand EBA bears some noticeable difference from that of the corresponding complexes where the ligands contain more rigid *m*-xylyl residues. Although both the dicopper(I) and dicopper-(II) complexes with EBA maintain a tendency to perform intramolecular reactions with small exogenous ligands, the long carbon chain is less easily adapted to the limited conformational mobility allowed by the arrangement imposed by small bridging ligands between the two copper centers. This feature was certainly anticipated at the outset, but we thought that higher ligand flexibility could be advantageous in catalysis. Comparing the activity of the dicopper(II) complexes of L-55, L-66 (ref 1), and EBA in the catechol oxidase reaction, we observe the followed trends:

first step:

$$[Cu_2(L\text{-}66)]^{4+} \gg [Cu_2(L\text{-}55)]^{4+} > [Cu_2(EBA)]^{4+}$$

second step:

$$[Cu_2(L\text{-}55)]^{4+} > [Cu_2(EBA)]^{4+} \gg [Cu_2(L\text{-}66)]^{4+}$$

The first step involves electron transfer between a presumably bridging catechol anion and the dicopper(II) centers. It is clearly dominated by the reduction potential of the Cu(II)/Cu(I) couple and is always faster than the second step. The latter step involves oxygenation of the dicopper(I) species, binding of the catechol to the Cu_2O_2 intermediate, and electron transfer from the catechol anion to the dioxygen moiety. For $[Cu_2(L\text{-}66)]^{2+}$ the slow reaction with dioxygen is the rate-determining step of the catalysis,[1] thus limiting the efficiency of the L-66 complex. By contrast, since oxygenation of $[Cu_2(L\text{-}55)]^{2+}$ and $[Cu_2(EBA)]^{2+}$ is very fast, the step limiting the overall catalytic process in these cases is the binding and the reaction of the catechol to the oxygenated species. The better efficiency of these complexes as catalysts is due to the small size of the chelate rings, which makes the oxygenated species more reactive and allows the incoming substrate to displace the weak axial nitrogen donor (structure II). Between the L-55 and EBA complexes the former

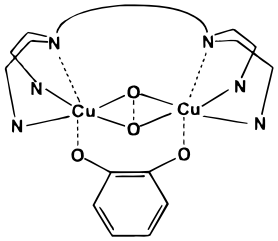

Structure II

is the most effective catalyst because the ligand is better suited to keep the folded structure, which facilitates binding of the bridging substrate, and does not suffer the inhibition process at high catechol concentration.

Experimental Section

All reagents were purchased from commercial sources and used as received unless noted otherwise. $[Cu(MeCN)_4]PF_6$ was prepared by a literature method[38] and recrystallized to analytical purity. Dimethylformamide was degassed and distilled under vacuum from calcium hydride. Acetonitrile for spectral measurements was successively distilled from potassium permanganate, sodium carbonate, and calcium hydride. The synthesis and manipulation of copper(I) complexes were performed with Schlenk techniques. Infrared spectra were recorded on a Jasco FT/IR-5000. Elemental analyses were performed at the microanalytical laboratory of the Chemistry Department in Milano. NMR spectra were recorded on Bruker AC-200 and DRX-300 spectrometers, operating at 200 and 300 MHz, respectively. Optical spectra were obtained on HP 8452A and 8453 diode array spectrophotometers. Electrospray ionization MS spectra were acquired using a Finnigan MAT system equipped with an ionic trap MS detector. Frozen solution EPR spectra were obtained with a Varian E-109 spectrometer equipped with a Stelar EPR3 system, version 941.0. Azide binding studies to the copper(II) complexes were performed by adding concentrated methanolic solutions of the ligand to solutions of the complex at 20 °C. The spectral data were analyzed as described previously[20,28] (for $[Cu_2(EBA)(H_2O)_4]^{4+}$) or in the Supporting Information (for $[Cu_2(EBA)(OH)_2]^{2+}$) to deduce equilibrium constants and the stoichiometry of formation of the adducts. The materials and apparatus for electrochemistry have been described elsewhere.[20] Cyclic voltammograms were recorded using either a BAS 100 A or a BAS 100 W electrochemical analyzer. All the potential values are referenced to a satured calomel electrode (SCE). Under the present experimental conditions, the one-electron oxidation of ferrocene occurs at +0.38 V.

1,6-Bis[[bis(1-methyl-2-benzimidazolyl)methyl]amino]-*n*-hexane (EBA) Dihydrate. A mixture of 1,6-hexanediamine (0.083 g, 0.71 mmol), 2-(chloromethyl)-1-methylbenzimidazole (0.54 g, 3.0 mmol),[20]

(32) Santagostini, L.; Gullotti, M.; Monzani, E.; Casella, L.; Dillinger, R.; Tuczek, F. Submitted for publication.
(33) Jameson, D. L.; O'Connor, C. J. *Inorg. Chem.* **1984**, *23*, 190.
(34) Sorrell, N. T.; Vankai, V. A.; Garrity, M. L. *Inorg. Chem.* **1991**, *30*, 207.
(35) Obias, H. V.; Lin, Y.; Murthy, N. N.; Pidkock, E.; Solomon, E. I.; Ralle, M.; Blackburn, N. J.; Neuhold, Y.-M.; Zuberbühler, A. D.; Karlin, K. D. *J. Am. Chem. Soc.* **1998**, *120*, 12960.
(36) Karlin, K. D.; Kaderli, S.; Zuberbühler, A. D. *Acc. Chem. Res.* **1997**, *30*, 139.
(37) Tolman, W. B. *Acc. Chem. Res.* **1997**, *30*, 227.
(38) Kubas, G. J. *Inorg. Synth*. **1979**, *19*, 90.

anhydrous sodium carbonate (0.16 g, 1 5 mmol), and acetonitrile (40 mL) was refluxed for 20 h and then left under stirring at room temperature. The crude product was evaporated to dryness under vacuum, and the residue was treated under stirring with 6 M aqueous hydrochloric acid (30 mL) for 5 min. The inorganic salts were filtered off, and the solution cooled in an ice bath was treated with excess concentrated ammonia under stirring. The white solid thus precipitated was filtered off, washed with small amounts of cold water and diethyl ether, and dried under vacuum (yield 60%). Anal. Calcd for $C_{42}H_{52}N_{10}O_2$: C, 69.20; H, 7.19; N, 19.22. Found: C, 69.78; H, 6,97; N, 19.36. IR (KBr, cm^{-1}): 3384 s, 3056 in, 2938 s, 2860 s, 1615 m, 1514 m, 1477 s, 1441 s, 1404 s, 1361 m, 1334 s, 1288 m, 1238 m, 1116 m, 1006 m, 988 m, 864 m, 770 s, 764 s, 656 w. ^{1}H NMR ($CDCl_3$): δ 1.20 (s, 4H, CH_2), 1.58 (s, 4H, CH_2), 2.70 (t, 4H, NCH_2), 3.72 (s, 12H, NCH_3), 4.12 (s, 8H, CH_2-benzimidazolyl), 7.2−7.3 and 7.7−7.8 (m, 16H, Ph).

$[Cu_2(EBA)][PF_6]_2\cdot 2CH_3CN$. To a degassed solution of the ligand (0.80 mmol) in methanol (30 mL) was added solid tetrakis(acetonitrile)-copper(I) hexaflurophosphate (1.7 mmol). The light yellow precipitate that immediately formed was left under stirring, under an Ar atmosphere. Then the precipitate was filtered, washed with a small portion of degassed tetrahydrofuran, and dried under vacuum. Anal. Calcd for $C_{46}H_{54}N_{12}Cu_2P_2F_{12}$: C, 46.35; H, 4.57; N, 14.10. Found C, 46.12; H, 433; N, 14.00.

$[Cu_2(EBA)(H_2O)_4][ClO_4]_4$. To a solution of the ligand (0.1 g, 0. 14 mmol) in 20 mL of chloroform/methanol, 1:1 (v/v), was added solid copper(II) perchlorate hexahydrate (0.11 g, 0.29 mmol). The blue-green solution was stirred for about 1 h at room temperature until spontaneous precipitation of the complex began. Precipitation was completed by adding a small amount of diethyl ether. The product was then filtered off, washed with small amounts of water and diethyl ether, and dried under vacuum. Anal. Calcd for $C_{42}H_{56}N_{10}O_{20}Cu_2Cl_4$: C, 39.11; H, 4.38; N, 10.86. Found: C, 39.38; H, 4.28; N, 10.80. IR (Nujol mull, cm^{-1}): 3538 m, 1653 m, 1616 m, 1533 m, 1504 m, 1325 w, 1296 m, 1093 vs sh, 981 w, 943 w, 914 w, 854 w, 750 s, 623 s. UV−vis [(MeOH/MeCN (9:1, v/v), λ_{max}, nm (ϵ, M^{-1} cm^{-1})]: 245 (29 700), 272 (33 400), 280 (33 700), 300 sh (2200), 350 sh (1000), 675 (280).

$[Cu_2(EBA)(OH)_2][PF_6]_2\cdot CH_3OH$. A solution of EBA (0.14 mmol) and tetrakis(acetonitrile)copper(I) hexafluorophosphate (0.282 mmol) in degassed methanol (40 mL) was stirred for 1 h under Ar, at room temperature, in a Schlenk flask. The mixture was then exposed to dioxygen (1 atm) for 1 h under stirring. The initial yellow solution quickly turned blue, and precipitation of the complex occurred. The product was filtered off, washed with a small amount of cold diethyl ether, and dried under vacuum. Anal. Calcd for $C_{43}H_{54}N_{10}O_3Cu_2P_2F_{12}$: C, 43.92; H, 4.63; N, 11.91. Found: C, 44.21; H, 4.18; N, 11.45. IR (Nujol mull, cm^{-1}): 3665 w, 3598 w, 1618 m, 1598 w, 1527 m, 1498 m, 1327 m, 1298 m, 1120 m, 1088 m, 1058 m, 1030 w, 1011 w, 973 m, 940 w, 926 w, 911 w, 840 vs, 746 s. UV−vis [MeOH/MeCN (1:1, v/v), λ_{max}, nm (ϵ, M^{-1} cm^{-1})]: 246 (30 600), 274 (33 000), 282 (27 600), 310 (5100), 354 (6500), 550 sh (170), 610 (180).

$[Cu_2(EBA)(N_3)(H_2O)_2][ClO_4]_3$. This compound was prepared by mixing equimolar solutions of $[Cu_2(EBA)(H_2O)_4][ClO_4]_4$ (0.05 g, 0.039 mmol) in acetonitrile (5 mL) and sodium azide (0.04 mmol) in a minimum amount of methanol. The resulting dark green solution was treated with diethyl ether and left standing in a refrigerator until precipitation of the adduct occurred. This was then collected by filtration, washed with small amounts of cold water and diethyl ether, and dried under vacuum. Anal. Calcd for $C_{42}H_{52}N_{13}O_{14}Cu_2Cl_3$: C, 42.16; H, 4,38; N, 15.22. Found: C, 42.03; H, 4.22; N, 15.43. IR (Nujol mull, cm^{-1}): 3618 m, 3541 m, 2048 s, 1618 w, 1504 m, 1483 m, 1321 w, 1294 w, 1095 vs sh, 1010 w, 939 w, 750 s, 623 s. UV/vis [MeOH/MeCN (7:3, v/v), λ_{max}, nm (ϵ, M^{-1} cm^{-1})]: 246 (26 000), 274 (30 100), 280 (29 000), 380 (2600), 440 sh (1500), 640 (400), 740 sh (350).

A small sample of the azide adduct was prepared similarly using unsymmetrically labeled sodium azide ($^{15}N^{14}N^{14}N$, 99% ^{15}N; Cambridge Isotope Laboratories, Woburn, MA). The IR spectrum of this compound was identical with that of the unlabeled compound except for the position of the azide band.

Caution! *Although the perchlorate complexes reported in this study were not found to be shock sensitive, the materials should be handled with care and in small quantities.*

Potentiometric Determinations. Potentiometric determinations of EBA in the absence and in the presence of copper(II) ions were performed with an apparatus and methods described elsewhere[1] in 50 mL of an acetonitrile/water, 80:20 (v/v), mixture made 0.1 M in ionic strength with $NaClO_4$ at 298 K. The electrodes were dipped for more than 1 h in the above solvent mixture before standardization of the system, which was also made as previously described.[1] The HYPERQUAD[39] program was used to process the data to calculate both the protonation and stability constants.

Single-Crystal X-ray Structure Determination of $[Cu_2(EBA)(OH)_2][PF_6]_2$. The crystals of the dicopper(II) complex of EBA used in X-ray analysis were grown by slow evaporation of a methanol solution obtained by air oxidation of $[Cu_2(EBA)][PF_6]_2$. Despite many attempts, we were not able to obtain single crystals suitable for collecting data using conventional X-ray sources. Furthermore, the crystals lose crystallinity under long exposure to the X-ray beam, even when sealed in a glass capillary tube. These problems were largely overcome by collecting data using synchrotron radiation at the ELETTRA X-ray diffraction beamline. Diffraction data collected at 100 K enabled us to solve and refine the structure, despite the poor quality of the crystal, due mainly to the disorder of the PF_6^- groups, which, even at the low temperature of data collection, lowered the number of reflections at high θ angles. The rotation method was used. A light-blue crystal of dimensions 0.4 × 0.3 × 0.2 mm was mounted on a glass capillary, and data were collected at 100 K with a wavelength of 0.90 Å and a Mar Research imaging plate (300 mm) at a distance of 100 cm. The exposure time for each frame was 60 s. A total of 2695 independent reflections were collected, 2509 of which, having $I > 2\sigma(I)$, were used in the subsequent calculations. A lowering of the reflection intensity with increasing θ Bragg angle was apparent. Unit cell parameters are $a = 22.458(2)$, $b = 10.728(1)$, and $c = 19.843(2)$ Å for the orthorhombic $Pca2_1$ space group, $V = 4780.8(8)$ Å^3, $Z = 4$, $M_w = 1143.9$, and $D_{calcd} = 1.59$ g cm^{-3}. Data were reduced by the program MOSFLM 6.0.[40] The structure was solved by conventional Patterson and Fourier methods and refined by the least-squares method.[41,42] The noncentrosymmetric space group was clearly indicated by the peak distribution in the Patterson map and by the final refinement. The latter leads to cationic species that present an approximately 2-fold axis, which, however, does not relate the two crystallographically independent PF_6^- anions. During the refinement the planar geometry of the methylimidazole groups and the octahedral environment of the PF_6^- groups were constrained. The final refinement of 240 parameters (137 restrains), treating anisotropically only the Cu and P species and including the H atom contribution, held constant, gave an R index of 0.089 ($R_w = 0.23$). Complete tables of atomic parameters and bond lengths and angles are included as Supporting Information.

Kinetics of 3,5-Di-*tert*-butylcatechol Oxidation. The reactions were studied in a magnetically stirred and thermostated cell with 1 cm path length at 20 ± 0.1 °C. The solvent employed for the kinetics was a 30:1 (v/v) mixture of methanol/aqueous phosphate buffer (50 mM), pH 5.1, saturated with atmospheric oxygen. In the study of the dependence of the oxidation rate on DTBC concentration, the concentration of $[Cu_2(EBA)]^{4+}$ catalyst was kept at 14 μM, while that of the substrate was varied from 0.07 to 15 mM. The formation of DTBQ was followed through the development of the corresponding band at 396 nm (ϵ 1500 M^{-1} cm^{-1}). The noise during the measurement was reduced by reading the difference in absorbance between 396 and 800 nm (at 800 nm the absorbance variation during the reactions is due only to noise). In all cases the reactions showed a biphasic behavior. Since the two steps were usually not well separated, the initial reaction

(39) Sabatini, A.; Vacca, A.; Gans, P. *Coord. Chem. Rev.* **1982**, *120*, 389.
(40) Leslie, A. G. W. MRC Laboratory, Cambridge, 1998.
(41) Sheldrik, G. M. SHELXL-86, Program of Structure Solution. *Acta Crystallogr., Sect. A* **1990**, *46*, 467.
(42) Sheldrik, G. M. SHELXL-93, Program for Structure Refinement, Universität Göttingen, Göttingen, Germany, 1993.

rates for both phases were obtained by fitting the dependence of the absorbance vs time using an equation describing two consecutive reactions in the catalytic cycle, as described in the Supporting Information. In the set of experiments aimed at studying the effect of pH on the rates, the pH of the buffer solutions added to the methanol was varied from 3.4 to 5.3; the catalyst concentration was 14 μM, and the substrate concentration was kept at 6 or 1.5 mM. The exact pH of the methanol/aqueous buffer solution, 30:1 (v/v), was determined by calibrating the electrode through the addition of measured quantities of standard perchloric acid solution to a CH_3OH/H_2O solution, 30:1 (v/v), according to Gran's method.[31]

Effect of Hydrogen Peroxide on the Kinetics of DTBC Oxidation. The effect of hydrogen peroxide on the reaction rates was studied using the same solvent mixture as before, saturated with atmospheric oxygen. The concentration of the catalyst was 14 μM, that of DTBC was 6 mM, and that of hydrogen peroxide was varied from 0.04 to 0.6 mM. The reaction shows a biphasic behavior as in the absence of the peroxide; both the rates of the two phases are influenced by H_2O_2 in a concentration-dependent manner.

Experiments for the Detection of Hydrogen Peroxide during the Catalytic Cycle. The presence of hydrogen peroxide in the reaction mixture was analyzed by using the iodimetric assay based on I_3^-, which has a characteristic absorption band at 353 nm (ϵ 26 000 M^{-1} cm^{-1} in water).[43] When a solution of methanol/aqueous phosphate buffer (50 mM), pH 5.1, 30:1 (v/v), saturated with potassium iodide and atmospheric oxygen is stirred, the I_3^- band develops very slowly. The addition of 0.2 mM hydrogen peroxide gives rise to a fast growth of the I_3^- band. Even in the presence of the large amount of methanol in the solvent mixture, the rate of the reaction is strongly accelerated by the enzyme lactoperoxidase (10 nM), so that in all experiments for the detection of peroxide the enzyme was always introduced. When the catechol oxidation reaction is performed in the iodide-saturated mixed solvent containing 14 μM $[Cu_2(EBA)]^{4+}$, 6 mM DTBC, and 10 nM LPO, the quinone absorption band develops with the same rate as observed in the absence of I^- and LPO. At the same time the I_3^- band slowly develops but with a rate that does not differ significantly from that of autoxidation in the mixed solvent used. The addition of 0.2 mM H_2O_2 gives rise to a fast oxidation of iodide.

Catalase Activity Assay of $[Cu_2(EBA)]^{2+}$. In this experiment the capability of hydrogen peroxide to oxidize the dicopper(I) complex of EBA was studied in deoxygenated solvent and in the presence of iodide, which acts as a competitive reducing agent. The experiment was performed with deoxygenated solvent under an argon atmosphere and at 20 °C using the equipment for low-temperature spectra. A mixture of methanol/aqueous phosphate buffer (50 mM), pH 5.1, 30:1 (v/v), saturated with potassium iodide and containing 10 nM LPO and 21 μM $[Cu_2(EBA)][PF_6]_2$, was treated with 23 mM hydrogen peroxide. The addition of the peroxide produces a fast development of the I_3^- band, while the complex remains in the reduced state since no appreciable optical change occurs in the d−d region.

Stoichiometry of Catechol Oxidation. This experiment was performed in an optical cell (1 cm path length) equipped with a Schlenk connection. To a degassed solution of $[Cu_2(EBA)]^{4+}$ (final concentration 14 μM) in methanol/aqueous buffer 50 mM, pH 5.1, 30:1 (v/v), was added anaerobically a concentrated solution of DTBC (final concentration 10 mM) in the same solvent (total volume 1.56 mL). A small amount of air-saturated methanol (40 μL) was added via gas-tight syringe, and the formation of DTBQ was followed spectrophotometrically at 396 nm until all dioxygen was consumed. The catalyst was in the reduced form at the end of the reaction. From the solubility of O_2 in methanol (2.5 mM at 25 °C)[44] and the absorbance increase at 396 nm, after the amount of DTBQ produced by reduction of the catalyst was subtracted, the stoichiometry of the reaction was found to be exactly 2 catechol:1 O_2.

Titration of $[Cu_2(EBA)(OH)_2][PF_6]_2$ with Perchloric Acid. To a 86 μM solution of the complex in $CH_3CN/MeOH/H_2O$, 6:3:1 (v/v/v), was added in several steps perchloric acid. The exact pH of the mixture was determined by calibrating the electrode through standard acid/base additions according to Gran's method. Starting from pH 8, the UV−vis spectrum of the solution was recorded after each addition of acid until the pH reached the value of 3.4.

Low-Temperature Spectroscopy. The low-temperature spectra (−78 °C) recorded during oxygenation of $[Cu_2(EBA)]^{2+}$ and $[Cu_2(L\text{-}66)]^{2+}$ [32] were obtained with a custom-designed immersible fiber-optic quartz probe (Hellma) fitted to a Schlenk vessel and connected with a HP 8452A diode array spectrophotometer. The experiments were performed in acetone since the solubility of the complexes in other suitable solvents (THF, CH_2Cl_2) was too low. Identical results were obtained by exposing a cooled anaerobic solution of the $[Cu_2(EBA)]^{2+}$ complex to dioxygen (1 atm) or adding the Cu(I) complex to a preoxygenated solution at low temperature.

Acknowledgment. We thank the Italian Murst and the CNR staff at ELETTRA, Trieste, Italy, for helping during measurements at the Crystallographic Beamline supported by CNR and Sincrotrone Trieste. We greatly appreciate the assistance of Dr. Luca Gianelli in performing MS spectral analysis. P.Z. gratefully acknowledges the financial support of the University of Siena.

Supporting Information Available: Text describing the procedure for estimating pK_a values of nonseparable proton dissociation equilibria and binding constants of simultaneous azide binding equilibria and the kinetic treatment of a catalytic cycle with two consecutive steps, Table S1 giving CV parameters for the reduction of $[Cu_2(EBA)]^{4+}$−azide complexes, and Figures S1 and S2 showing cyclic voltammetric responses of $[Cu_2(EBA)(OH)_2]^{2+}$ and $[Cu(2\text{-}BB)]^{2+}$. Complete tables of atomic parameters and bond lengths and angles are available in CIF format. This material is available free of charge via the Internet at http://pubs.acs.org.

IC990397B

(43) Jenzer, H.; Jones, W.; Kohler, H. *J. Biol. Chem.* **1986**, *261*, 15550.

(44) Tokunaga, J. *J. Chem. Eng. Data* **1975**, *20*, 41.